Earth and Sun Systems Laboratory (ESSL)
Fiscal Year 2005 Science and Program Highlights

"Retrospective" trend simulations using the Whole Atmosphere Community Climate Model (WACCM)

The recently completed version 3 of the model (WACCM3) has been used to study the evolution of temperature and chemical composition since 1950, to help interpret trends brought about by changes in chlorine loading and greenhouse gases. Successful simulation of these trends is a prerequisite for using the model to predict future changes in the atmosphere, as greenhouse gases continue to increase while anthropogenic emissions of chlorine and bromine compounds decrease.

The figure below shows a comparison of the model-calculated ozone trend for 1979-2000 with the trend calculated from SAGE-I and SAGE-II satellite data. The agreement is generally very good, both as regards the morphology of the trend and, in most locations, its magnitude. These results suggest that there are no major omissions in our current knowledge of stratospheric photochemistry. Results for temperature trends (not shown) are also in good agreement with observations.

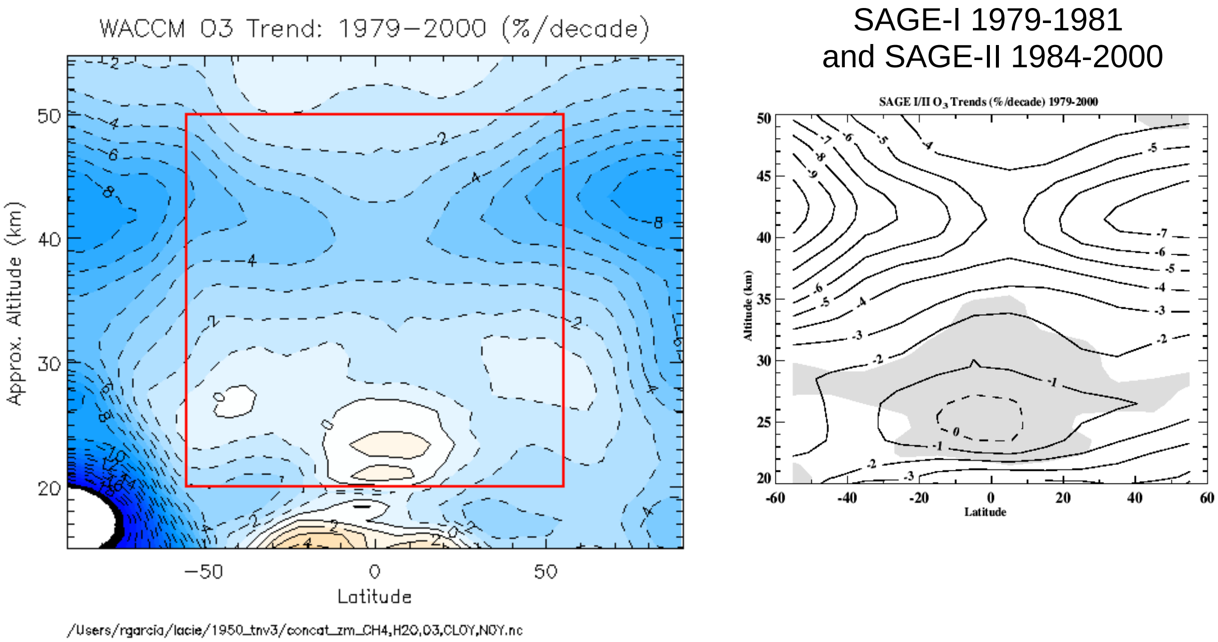

Fig. 1. Calculated (left) and observed (right) ozone trend for the period 1979-2000. The area outlined in red on the left panel corresponds to the region of the atmosphere for which trends can be computed from SAGE satellite observations (right).

NCAR Analysis Shows Widespread Pollution from 2004 Wildfires (link: http://www.ucar.edu/news/releases/2005/wildfires.shtml)

June 29, 2005

BOULDER—Wildfires in Alaska and Canada in 2004 emitted about as much carbon monoxide as did human-related activities in the continental United States during the same time period, according to new research by the National Center for Atmospheric Research (NCAR). The fires also increased atmospheric concentrations of ground-level ozone across much of the Northern Hemisphere.

A fire fighter works the line during the 2004 Alaska Solstice Complex fire. (Photo courtesy the Alaska Fire Service.)

The NCAR study, which indicates the extent to which wildfires contribute to atmospheric pollution, was published this month in Geophysical Research Letters. The researchers used a novel combination of observing instruments, computer models, and numerical techniques that allowed them to distinguish between carbon monoxide coming from the wildfires and from other sources.
The team concluded that the Alaskan and Canadian wildfires emitted about 30 teragrams of carbon monoxide from June through August of last year. Because of the wildfires, ground-level concentrations of ozone increased by 25% or more in parts of the northern continental United States and by 10% as far away as Europe.
"It is important to see how the influence of these fires can reach large parts of the atmosphere, perhaps even over the entire Northern Hemisphere," says NCAR scientist Gabriele Pfister, the study's lead author. "This has significant implications as societies take steps to improve air quality."

Carbon monoxide, a toxic gas that can affect human health even at low levels, is emitted by wildfires as well as by motor vehicles, industrial facilities, and other sources that do not completely burn carbon-containing fuels. Ground-level ozone, which affects human health in addition to damaging plants and influencing climate, is formed from reactions involving atmospheric pollutants, including carbon monoxide, in the presence of sunlight. Both pollutants are monitored by the Environmental Protection Agency. However, scientists have been unable to precisely determine regional emissions of carbon monoxide or the extent to which human and natural activities contribute to atmospheric concentrations of the gas.

Wildfires in Alaska and western Canada were particularly intense in the summer of 2004, largely because of unusually warm and dry weather. To quantify carbon monoxide emissions from the fires, the research team used a remote sensing instrument known as MOPITT (Measurements of Pollution in the Troposphere) that is operated by NCAR and the University of Toronto and flown on NASA's Terra satellite. The scientists simulated the transport of the pollutants emitted by the fires and the resulting production of ozone with an NCAR computer model called MOZART (Model for Ozone and Related Chemical Tracers).

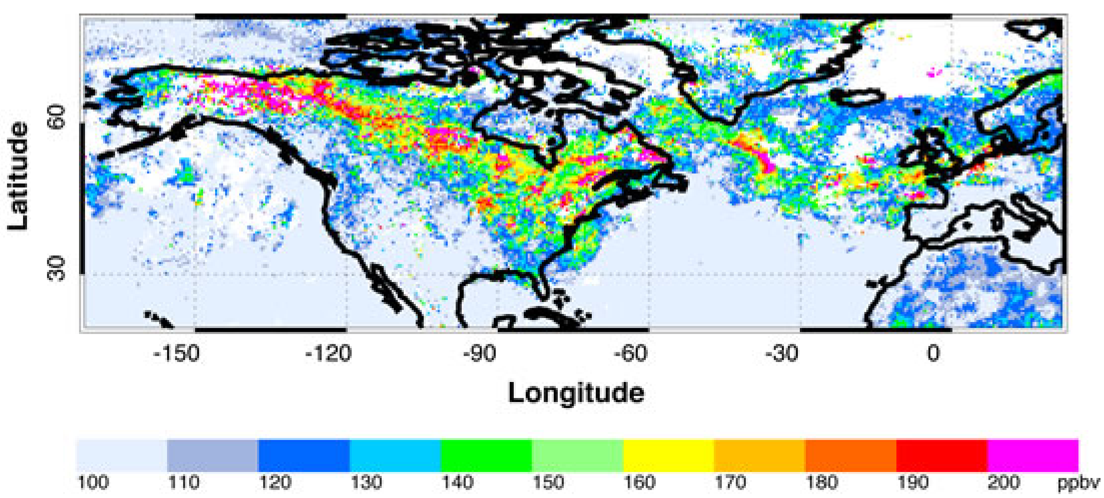

This MOPITT image shows plumes of carbon monoxide streaming from Alaskan fires across North America and the Atlantic during mid-July 2004. (Image courtesy the NCAR MOPITT Team.)

The team confirmed its results by using numerical techniques to compare simulated concentrations of carbon monoxide in the atmosphere with measurements taken by MOPITT. The researchers were able to get further confirmation by analyzing data from aircraft-mounted instruments that were taking part in a field project over North America and Europe. Pfister says the team is continuing to look at data taken last year at observing stations as far away as the Azores in order to track the movement of carbon monoxide and ozone from the wildfires. As a follow-up, she and other scientists plan to use a similar combination of observations, modeling, and numerical techniques to look at both natural and human-related emissions of carbon monoxide in South America.

Simulating the Climate of the Late Permian, Jeffrey T. Kiehl and Christine A. Shields

One of the more intriguing time periods in Earth's history is the boundary between the Permian and Triassic periods at 251 Ma. This boundary marks the largest extinction recorded in Earth's history, where across this boundary approximately 95% of marine and terrestrial species were lost. Associated with this event was an extended period of magma activity and extended ocean anoxia. What caused such a catastrophic change in life? A number of hypotheses have been proposed to explain various aspects of the extinction and climate of this time period. No one hypothesis can explain all of the paleo information for this period. Although a number of climate model simulations have been carried out for this period no fully coupled climate model simulation has existed for this time period. Fully coupled climate models are required to accurately simulate the ocean circulation, since using specified ocean boundary conditions highly constrains the climate solution and does not allow for a coupling of atmospheric and land hydrological processes to the ocean, e.g. input of fresh water to the ocean.

We have carried out the first realistic fully coupled climate simulation of this time period. We are using paleogeography conditions and specified CO_2 levels for this time period in the recently released CCSM3. The coupled simulation has been run for 2700 year, the longest continuous simulation of CCSM3, to date. The length of the simulation insures that the entire coupled system is in an equilibrium state.

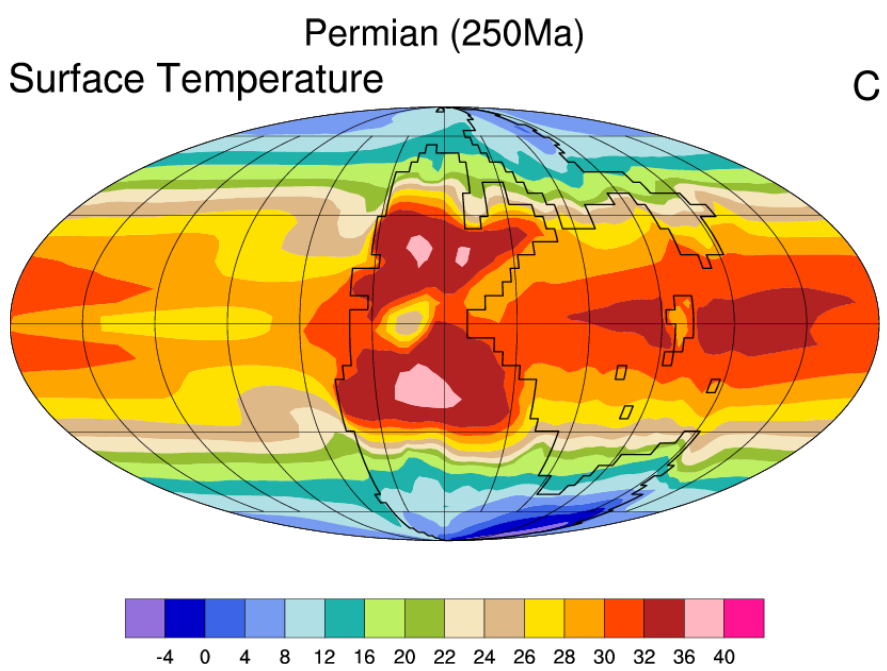

The above figure shows the annual mean surface temperature (°C) from years 2600 to 2700. The western tropical Panthalassic ocean has a warm pool of water with SSTs reaching 33 °C, compared to the present day western Pacific warm pool temperatures of 30 °C. The warmest regions over land occur in the subtropical desert regions.

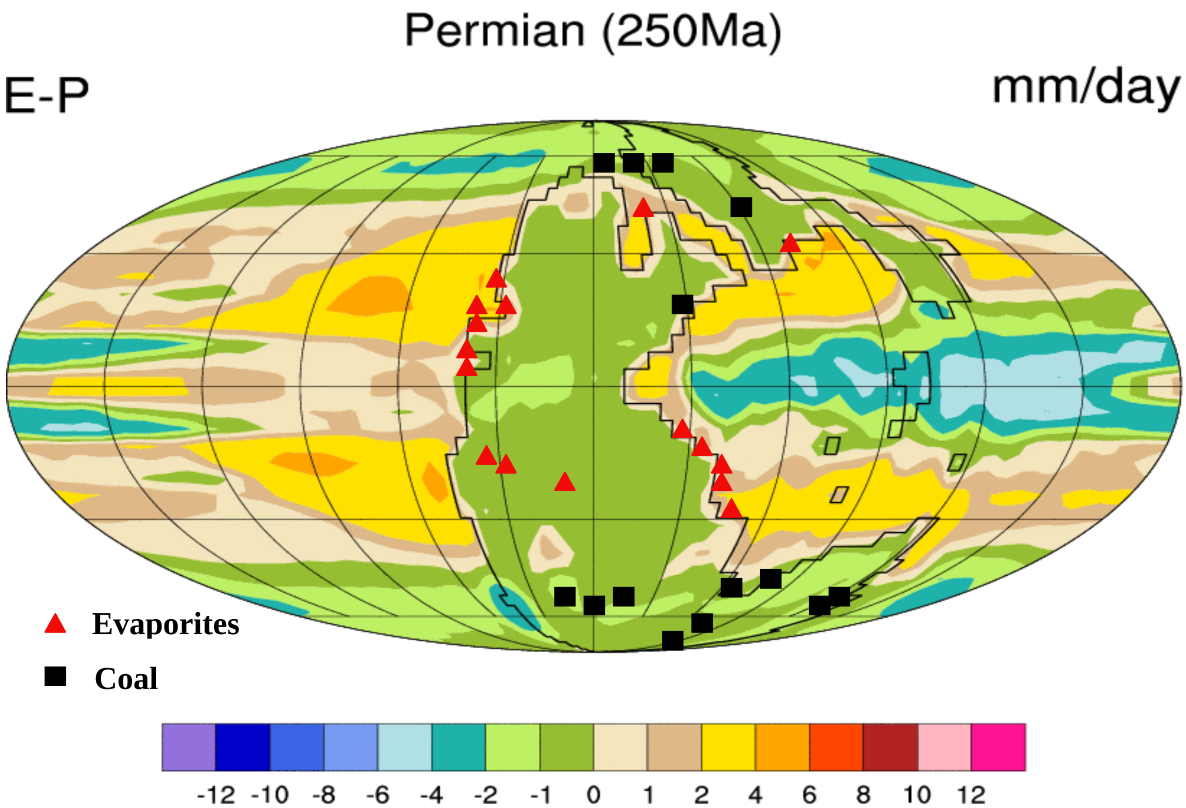

One metric of the climate of this time period comes from the geographic location of evaporite deposits. These occur in shallow water regions where the evaporation minus precipitation (E-P) is positive. The above figure shows the annual mean E-P from the CCSM3 simulation, with the observed location of evaporite deposits marked by red triangles. All but one of these observed evaporite sites matches the model simulation of the region of positive E-P.

An important observation of this time period is the indication that the oceans were anoxic for an extended period (~20 My) of time across the boundary. Low oxygen conditions could explain the limited marine life at this time. One hypothesis suggests that in a warm greenhouse climate with an associated low pole to equator thermal gradient, ocean mixing to depth would be limited due to strong stratification. Shown below is a map of ocean ideal age at 3000m. This is a measure of the last time water mass at this depth was at the ocean surface. Thus, it is a measure of how well mixed the ocean is at 3000m. The top figure is for the Late Permian simulation and one can see that the water is very old at this depth (~1000 years), indicating very poor mixing with the surface. This condition would lead to low oxygen levels in the ocean, thus supporting the hypothesis of global ocean anoxia. The present day solution indicates very efficient mixing in the ocean, unlike the Late Permian state.

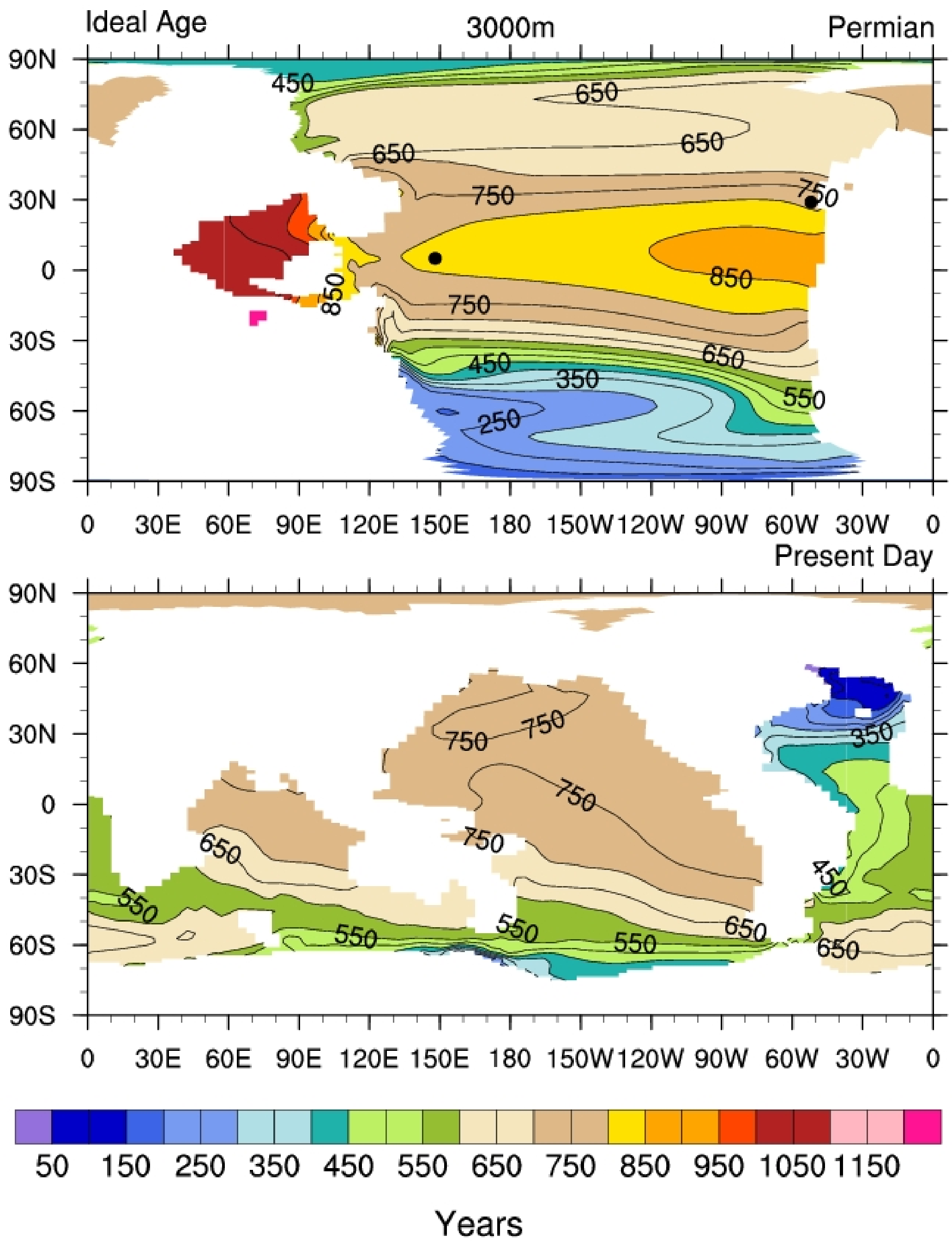

These findings indicate the need for substantial computational resources to explore the realm of deep time, where deep ocean time scales play a critical role in biogeochemical processes relevant to life on Earth.

Future efforts in exploring the climate of the Late Permian include: exploring the role of atmospheric chemical changes at this time including enhanced methane levels, fully coupled dynamic vegetation simulations and coupling of biogeochemical processes. As shown fully coupled climate models can now be applied to questions of climates in deep time. These types of models can be used to integrate observations and test scientific hypotheses. They can also serve as a catalyst for more synergistic collaborations on key climate issues.

Climate Change Commitment, Gerald A. Meehl, Warren M. Washington, William D. Collins, Julie M. Arblaster, Aixue Hu, Lawrence E. Buja, Warren G. Strand, and Haiyan Teng

Two global coupled climate models have been run in multi-member ensembles to show that if the concentrations of greenhouse gases had been stabilized in the year 2000, we are already committed to further global warming of about another half degree or close to 100% of the warming we have already experienced during the 20th century, and an additional 320% sea level rise from thermal expansion, or roughly three times the sea level rise that has already occurred, by the end of the 21st century (Fig. 1). At any given point in time, even if concentrations are stabilized, there is a commitment to future climate changes that will be greater than those we have already observed. These results show that the longer we wait, the more climate change we are committed to in the future.

(Meehl, G.A., W.M. Washington, W.D. Collins, J.M. Arblaster, A. Hu, L.E. Buja, W.G. Strand, and H. Teng (2005), How much more global warming and sea level rise? *Science*, *307*, 1769--1772.)

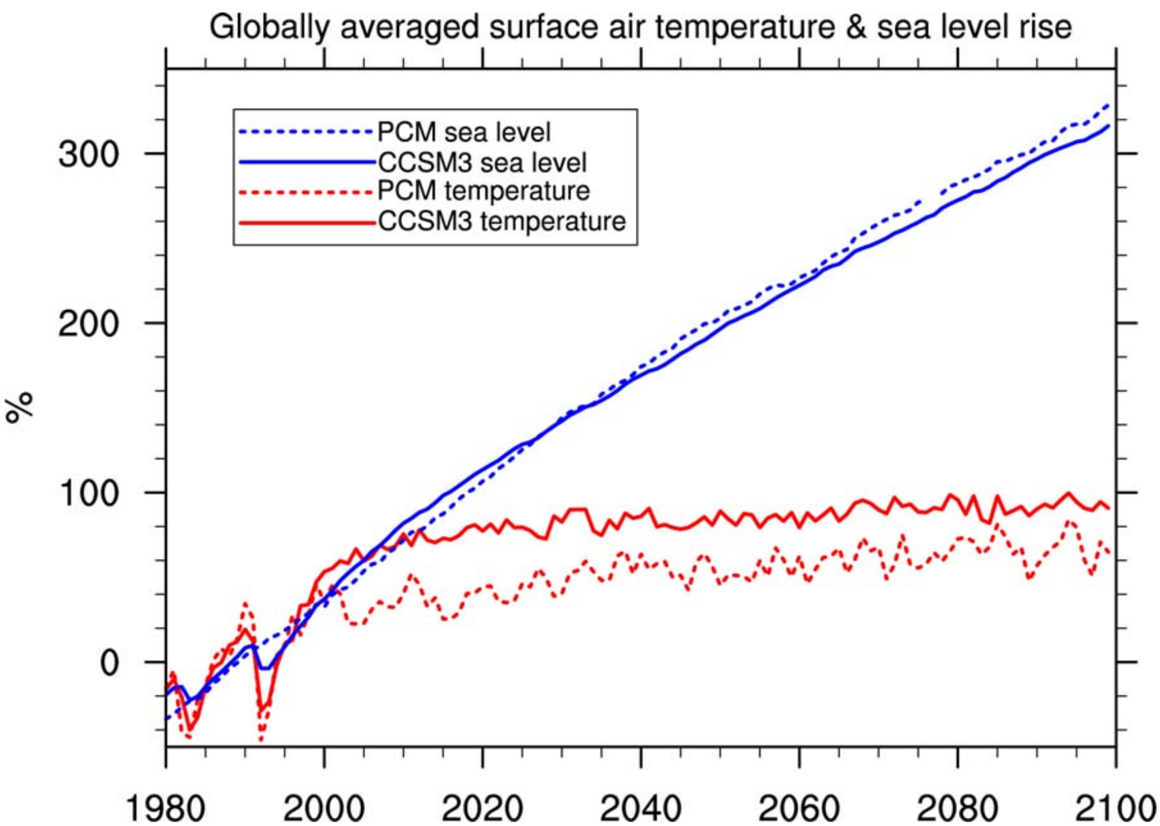

First order draft of Chapter 3, IPCC Fourth Assessment

A major new accomplishment in the Climate Analysis Section is the completion of the First Order Draft of Chapter 3 of the IPCC's Fourth Assessment AR4. Kevin Trenberth is a Coordinating Lead Author along with Phil Jones of the Climate Research Unit, University of East Anglia, U.K. Among the 62 Contributing Authors to the chapter were Jim Hurrell, Clara Deser, Aiguo Dai and Dennis Shea. The text is 108 pp singles spaced 11 point font. Of this the Executive Summary is 3 pp, the main text is 76 pp, including about 6 pages in the newly featured QACCS (Questions About Climate Change Science), 20 pages of references in abbreviated format and small (8.5) font, and 7 pp of Appendices. Fully 42 of the references are to papers by the CAS section. In addition there are 47 separate figures consisting of 111 panels (or individual plots), which includes 3 figures and 8 panels in the QACCS. All are reduced to single column or page width. Nearly all of the figures are new and have been redrafted and updated from original published sources, with over one third of those being done by Dennis Shea, at NCAR.

An example of a new innovative plot is given below. Here the previous characterization of the global mean temperature record as a linear trend of 0.6°C for the 20th century (red line) is seen to be a very poor fit to the actual annual mean values (black dots). Instead a better characterization is given by the blue line, which is a series of straight line fits to the data with breaks at 1920, 1940, and 1970. A linear trend is a reasonable fit only after about 1970 where it is seen that the warming amounts to 0.55°C in the past 34 years, and the overall warming is 0.75°C.

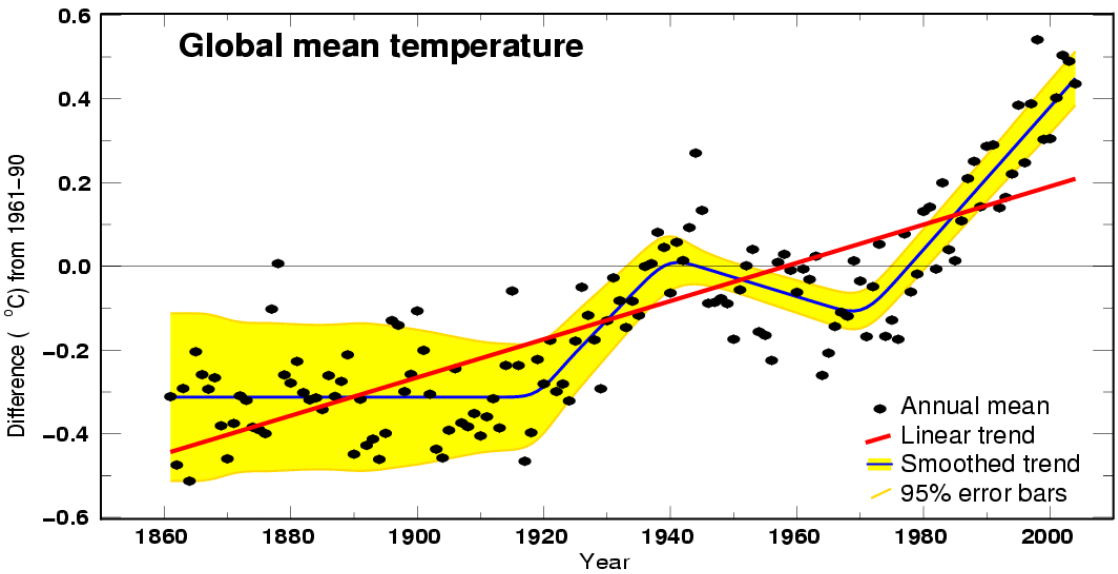

Multi-scale Hierarchical Organization of Tropical Convection

Figure 1 a shows the remarkable hierarchy of convective organization in the tropics: mesoscale convective systems (cloud clusters of scale ~100 km), families of mesoscale convective systems (superclusters of scale ~1000 km) and families of superclusters embedded in the tropical intraseasonal oscillation (a.k.a Madden-Julian Oscillation) whose scale is ~ 10,000 km (Nakazawa 1988).

Global models have difficulty in representing this multi-scale hierarchy. This vexing situation arises, at least in part, from uncertainties associated with convective parameterization. Contemporary parameterization does not take into account the organization of convection how it couples the large-scale environment. Advances in computer architecture now enable convective cloud systems to be represented *explicitly* in global models, presently in aquaplanet experiments. In “cloud-resolving convection parameterization” numerical cloud-system models are applied in global models in place of traditional convective parameterization, an approach that reveals MJO-like systems (Fig. 1b).

Multi-scale dynamical models are another recent development. By coupling analytic models of organized deep convection to equatorial beta-plane dynamics Moncrieff (2004) developed a non-linear mechanistic theoretical model that represents the scale-invariance and upscale effects of tropical convection. This model approximates the organized convective systems simulated by Grabowski’s super-parameterization, such as westward-tilt in the vertical and the meridional transport of zonal momentum (Figs. 1 c and d).

This type of work is highly relevant to THORPEX in regard to the two-way interaction between the large-scale organization of tropical convection and high-impact weather in mid-latitudes. Early THORPEX planning has shown that high-impact weather is frequently linked to the leading edge of Rossby wave trains triggered by tropical convection. Were global models to more skillfully represent the initiation and life-cycle of tropical convection there is prospect that planetary-wave teleconnection and synoptic-scale instability would be more accurately represented. This would a significant step towards improved probabilistic forecasts, if not improved prediction, of severe convective weather, heavy precipitation and intense winter cyclones in midlatitudes. The long-term objective is to use explicit numerical simulation and dynamical models to represent convective organization in parameterizations used in seasonal prediction models (ensembles of forecasts) and, ultimately, in climate models. Climate models have noted short-comings in the treatment of tropical convection. Note that for the foreseeable future it will be necessary to parameterize convection in these models since the explicit approach is prohibitive in computational respects.

Grabowski, W.W., 2001: Coupling cloud processes with the large-scale dynamics using the Cloud-Resolving Convection Parameterization (CRCP). *J. Atmos. Sci.*, **58**, 978-997.

Moncrieff, M.W., 2004: Analytic representation of the large-scale organization of tropical convection. *J. Atmos. Sci*., **61**, 1521-1538.

Nakazawa, T., 1988: Tropical superclusters within intraseasonal variations over the western Pacific. *J. Meteor. Soc. Japan*, **66**, 823-839.

Tomita, H., H. Miura, S. Iga, T. Nasuno, and M. Satoh, 2005: A global cloud-resolving simulation: Preliminary results from an aquaplanet experiment. *Geophys. Res. Lett.*, **32**, L08805.

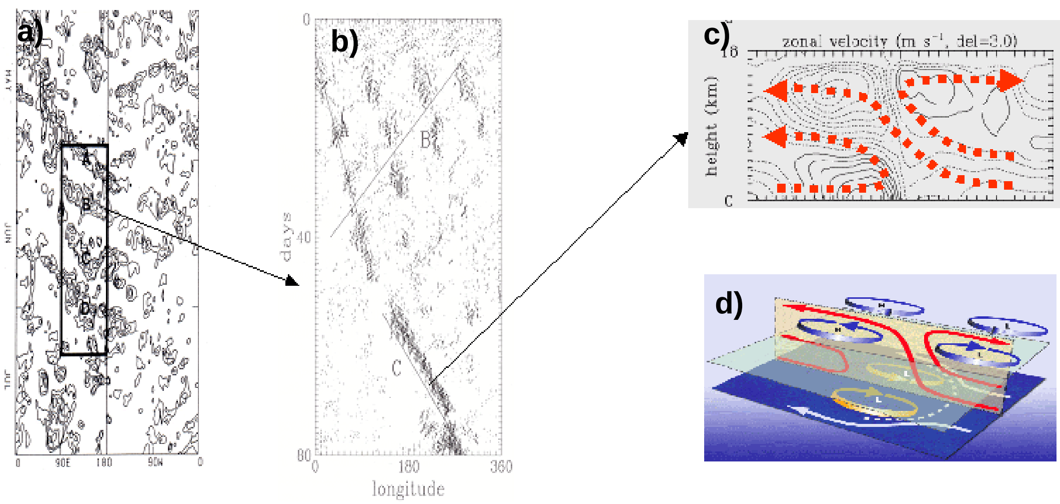

Figure 1. Hierarchical organization of tropical convection: a) a supercluster family measured as cold cloud tops in outgoing long-wave radiation measurements (Nakazawa 1988); b) supercluster family represented by cloud-resolving convection parameterization in an aquaplanet simulation (Grabowski 2001); c) vertical structure of the MJO-like system in Grabowski's simulation; and d) mechanistic dynamical model of the numerically simulated MJO-like system (Moncrieff 2004).

Water Cycle

Recent studies by Groisman et al. (2004) and others have shown an increasing trend in total mean cloudiness over the continental U.S. from 1960 – 1990 based on data collected by trained human observers. After 1990, many of the human observer sites were replaced by automatic ASOS stations that do not provide the same information as the human observer. U.S. military observation sites, however, continued to make manual cloud observations until the present time. Dai et al. (2006) utilized these observations to extend the results of Groisman et al. (2004) until 2004. Their results are consistent with the Groisman work, and show that mean total cloudiness over the U.S. Continent has increased by 2.9% per decade for the last 30 years (Fig.1). The analysis has shown that increasing cloudiness is also associated with a decrease in the diurnal temperature range, as to be expected: the main effect of cloud is to block the sun and reduce the maximum temperature.

The maximum increase in cloudiness is located in the mid-continental region of the U.S., where organized west-east traveling squall lines dominate the cloudiness (Figs. 2 and 3, Moncrieff and Liu 2005, Carbone et al. 2002), at least in the summer. These results suggest that there may be a trend towards increasing cloudiness due to enhanced squall line frequency or intensity. The analysis by Groisman et al (2004) shows an increasing trend of very heavy precipitation (95-100th percentile) of 6.5%/century, and an increase of 4.6%/century for thunderstorms during spring, which is consistent with this suggestions.

One mechanism that may lead to enhanced frequency or intensity of squall lines is an increase in water vapor mixing ratio at low levels in the atmosphere. Recent results from an analysis of column integrated water vapor by Trenberth et al (2005) shows an increase of water vapor over the global oceans of 1.3% per decade since 1988. Groisman's analysis using surface water vapor mixing ration over the U.S. shows an increase of 7.4% per century after 1950, consistent with the Trenberth analysis. This enhanced water vapor may help explain the observed increase in cloudiness and the enhanced heavy precipitation. To investigate this further, future water cycle research will examine the sensitivity of squall line generated cloudiness and precipitation to increased tropospheric water vapor.

Carbone, R.E., J.D. Tuttle, D. Ahijevych, S.B. Trier, 2002: Inferences of Predictability Associated with Warm Season Precipitation Episodes, *J. Atmos. Sci.*, **59**, 2033-2056.

Dai, A. 2006: Recent trends in cloudiness over the United States: A tale of monitoring inadequacies. Accepted in BAMS

Groisman, P.Y., R.Knight, T. Karl, D. Easterling, B. Sun, and J. Lawrence, 2004: Contemporary changes of the hydrological cycle over the contiguous United States: Trends derived from in-situ observations. *J. Hydromet*, **5**, 64 – 85.

Moncrieff, M. and C. Liu, 2005: Convective Organization in Prediction Models at ~10 km Grid-Resolution, Submitted to JAS.

Trenberth, K. J. Fasullo, and L. Smith, 2005: Trends and variability in column-integrated atmospheric water vapor. *Climate Dynamics*, **24**, 741 – 758.

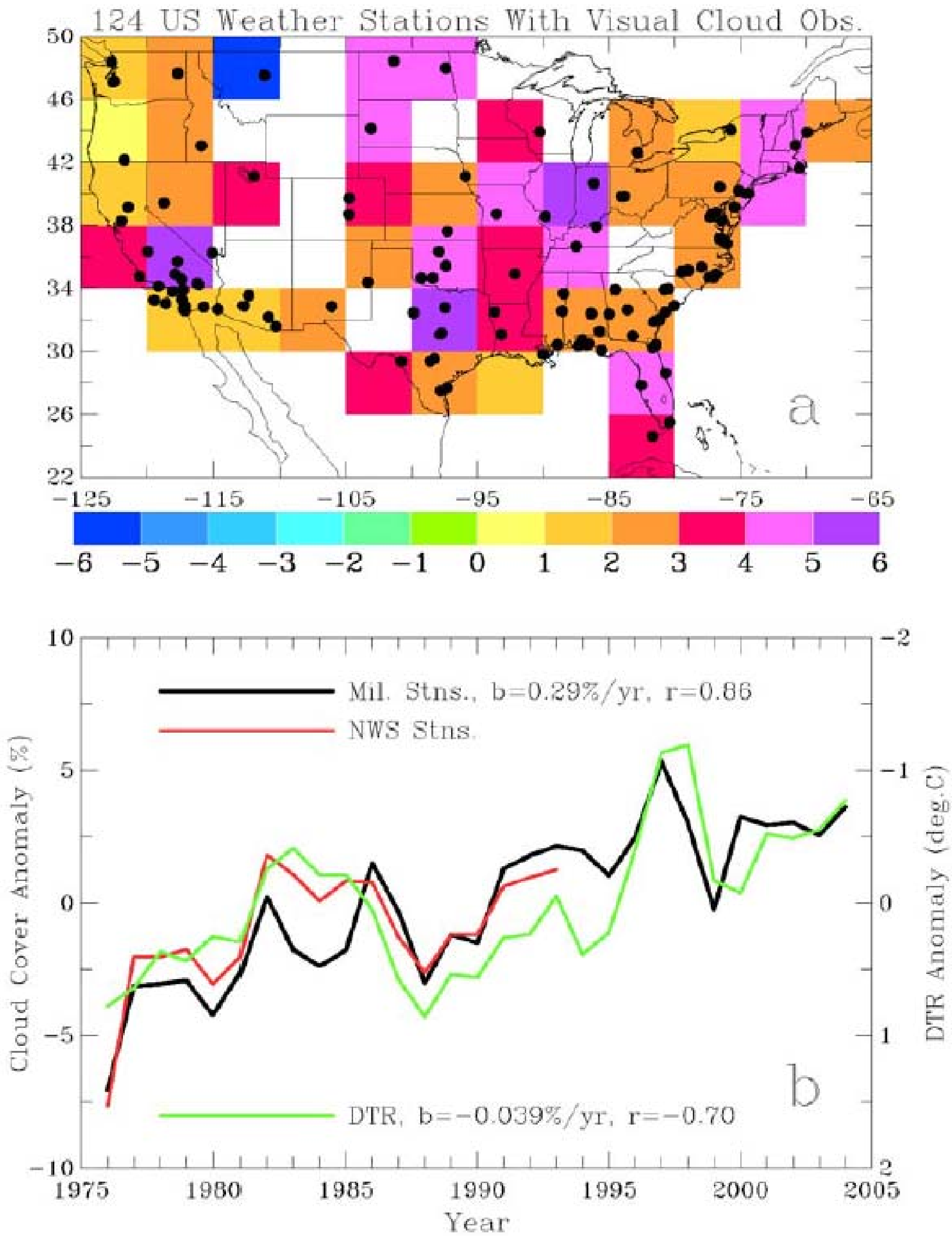

Figure 1 a. Distribution of 124 U.S. military weather stations (dots) with continuous human visual observations of total cloud, together with linear trends (color, % sky cover per decade) of annual total cloud cover during 1976-2004. b. Anomaly time series of annual total cloud cover averaged over the 4 degrees lat x 5 degrees lat boxes that have at least one of the stations shown in a (black line, b is it slope, and r is the correlation with the red line) and derived using all the NWS/FAA stations (red line, from 1976-1993 only.) Also shown is the diurnal temperature range (DTR) anomaly (green line, decreases downward on the right side ordinate, b is it slope and r is the correlation with the black line) averaged over the same areas with data in a using synoptic observations.

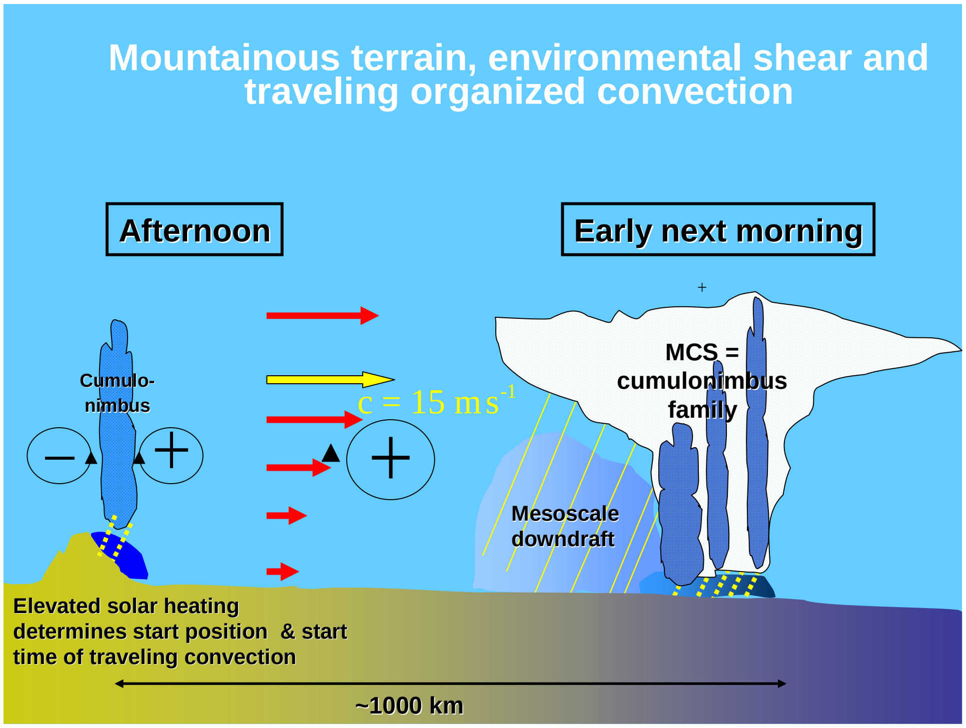

Figure 2 Schematic diagram of squall line formation and propagation over the continental U.S.

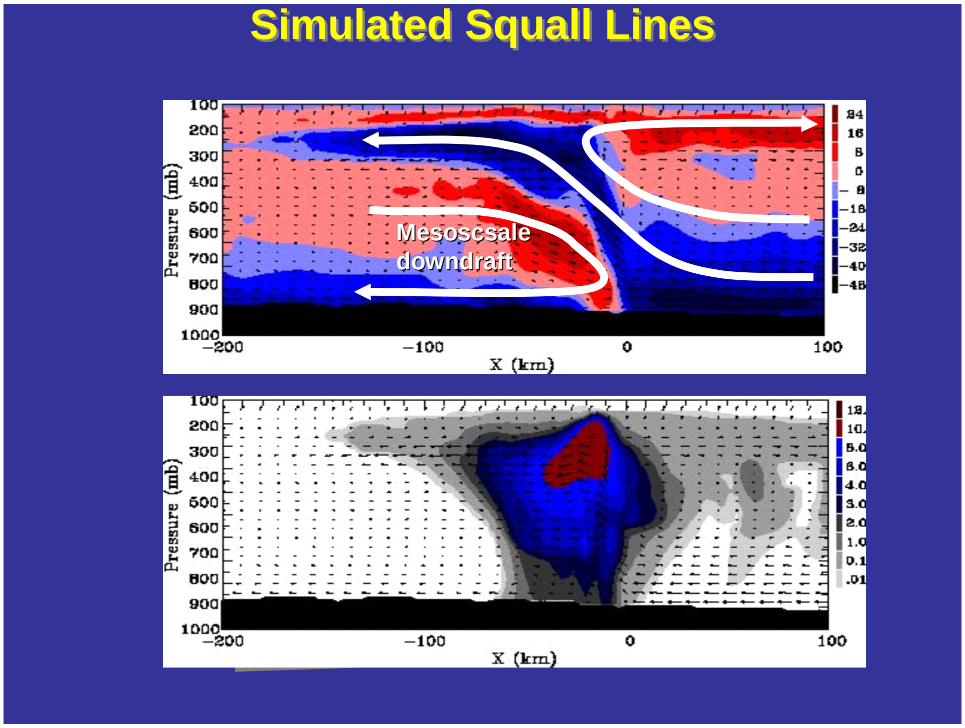

Figure 3 Squall line cross section for 3D simulation with 3 km horizontal resolution over the continental U.S.

Global Nitrogen Cycling at NCAR

In a collaborative effort across two NCAR divisions, CGD, ACD and NCAR's Biogeosciences program within TIIMES program, considerable research effort was devoted to the global nitrogen cycle. Highlights of this effort include completion of phase 1 the Santa Fe project funded through a director's opportunity fund (Scientific Analysis (of) Nitrogen (Cycle) Towards Atmospheric Forcing Estimation (Lamarque et al. 2005) , development of the terrestrial biogeochemistry code for N within the CCSM (P.E.Thornton) , release of a US N Science plan (Holland et al. EOS, volume 86(27) July 5, 2005, http://www.essl.ucar.edu/times/nsp/NSciPlan_Nov2004.pdf), publication of a long-term effort on the comparison of atmospheric N budgets for the US and Western Europe (Holland et al. 2005) and the release of two public access N data sets http://www-eosdis.ornl.gov).

Lamarque, J.F. J. Kiehl, G. Brasseur, T. Butler, P. Cameron-Smith, W.D. Collins, W.J. Collins, C. Granier, D. Hauglustaine, P. Hess, E. Holland, L. Horowits, M. Lawrence, D. McKenna, P. Merilees, M. Prather, P. Rasch, D. Rotman, D. Shindell, and P. Thornton. Assessing future nitrogen deposition and carbon cycle feedback using a multi-model approach. Part 1: Anaysis of nitrogen deposition. In press JGR-Atmospheric Chemistry.

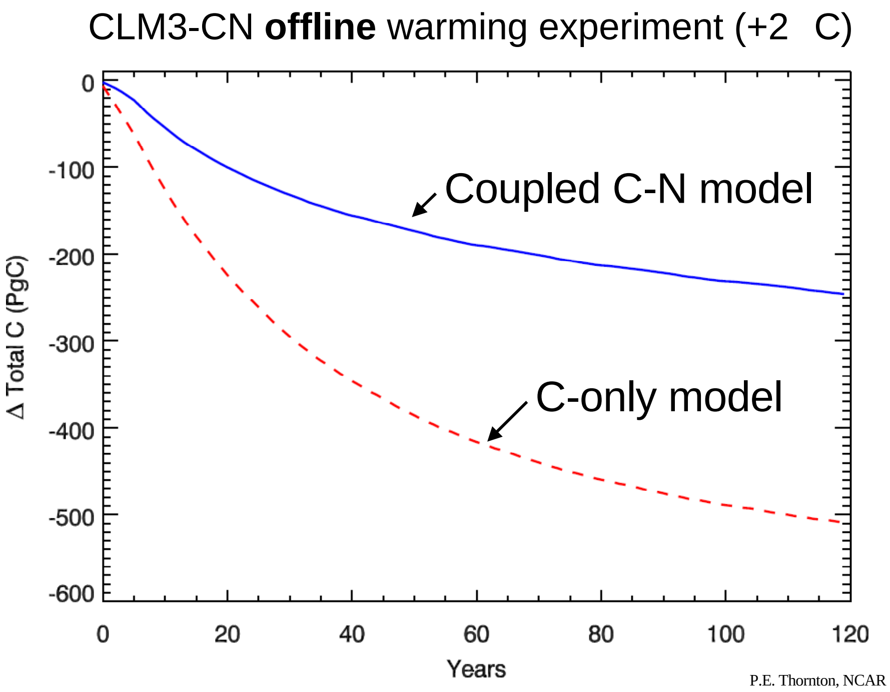

Simulated net global terrestrial carbon release using a carbon model and a coupled carbon nitrogen model. The simulations were done using the Community Land Model (Bonan version 3.0 modified to include carbon and carbon and nitrogen, Thornton 2005). The simulation was a step function 2 °C increase in temperature forcing of the model applied after a spin-up of the carbon or carbon nitrogen model.

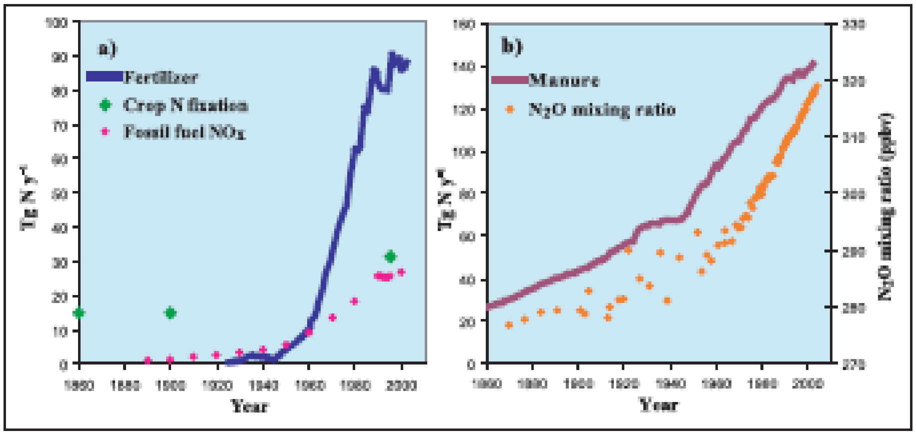

Fig. 1. (a) Changes in fluxes of reactive, or biologically available, N. (b) The simultaneous increase in atmospheric N2O concentrations, and increased manure production as a result of reactive N generation in Figure 1a. The Haber-Bosch process for the creation of fertilizer from N2 was invented in 1913. For data

sources, see http://www-eosdis.ornl.gov/. Published in EOS 86(27), Holland *et. al.)*

Holland, E. A., **B. H. Braswell**, J. Sulzman, and J.-F. Lamarque, Nitrogen deposition onto the United States and western Europe: synthesis of observations and models, Ecol. Appl., 2005

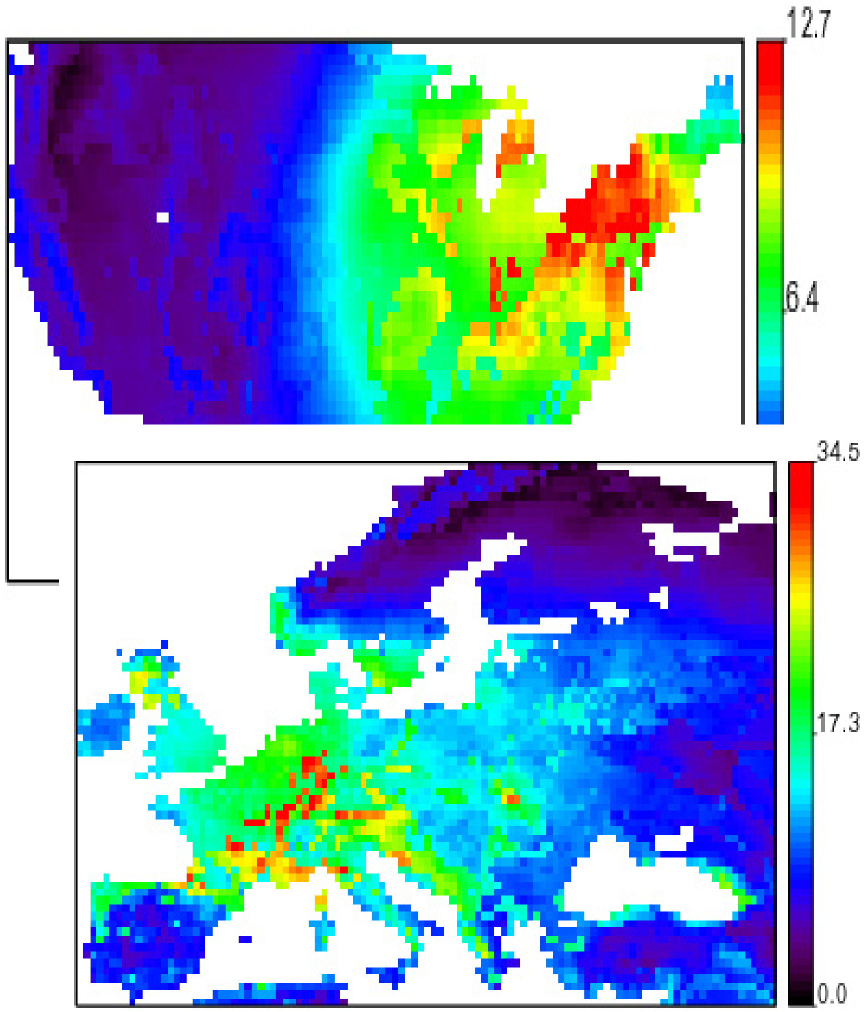

Estimated N deposition fluxes summed and integrated over the conterminous United States (top) and Western Europe (bottom). The N species considered for Europe were wet deposition of NH_4^+-N and NO_3^- -N, and dry deposition of HNO_3-N (g) (using the *V*d for HNO_3(g), NO2 (g), and particulate NH_4 . The area of the conterminous United States is 31.01 • 10^6 km^2 compared to 35.7 • 10^6 km^2 in continental Western Europe (excluding some of the small islands of the Norwegian archipelago and portions of Eastern Europe outside the measurement network). The mapped fluxes are available online http:www-eosdis.ornl.gov/.

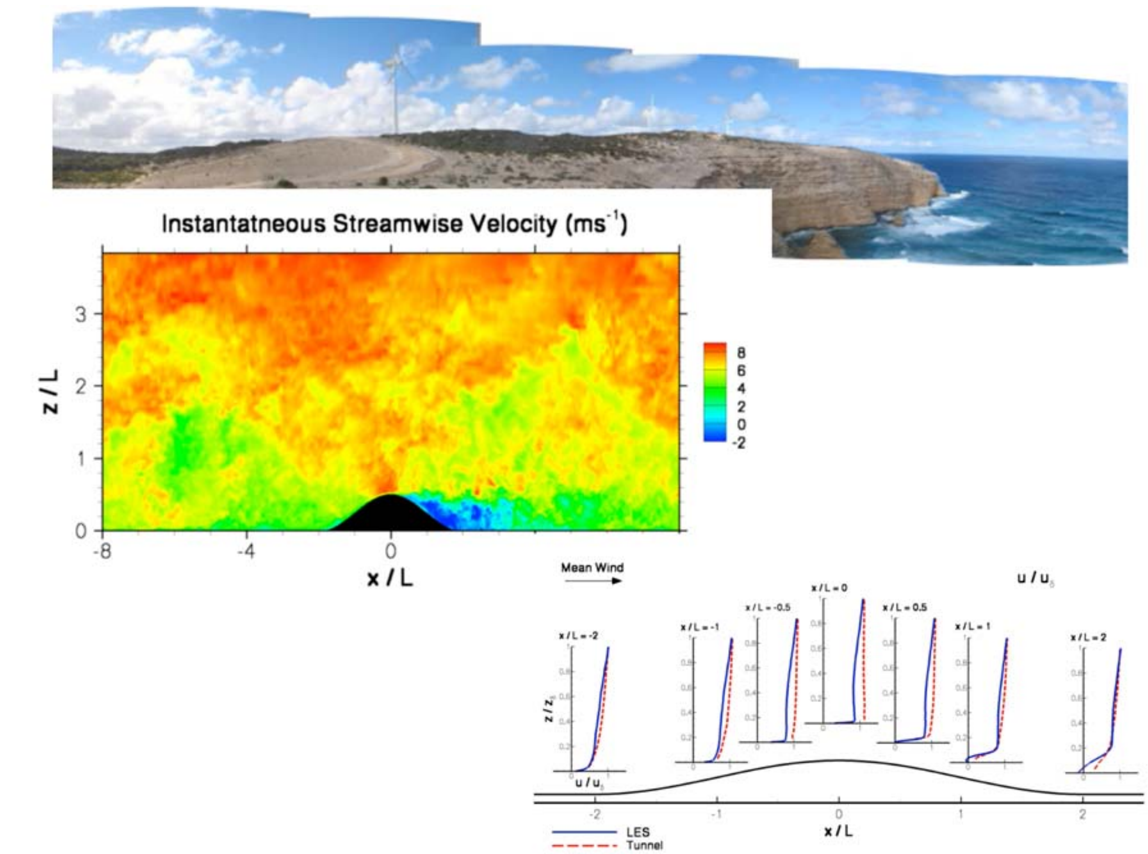

Figure 1: Results from turbulence resolving calculations of flow over a two-dimensional ridge with application for wind energy turbine design and deployment strategy. Top panel: Sample deployment location. Middle panel: Instantaneous slice of streamwise velocity showing strong spatial wind speed fluctuations induced by the topography. Bottom panel: Comparison of numerical predictions of streamwise velocity with wind tunnel observations.

MMM scientists, Edward Patton and Peter Sullivan, are using their newly developed large-eddy simulation code to aid in the design and deployment of wind energy turbines. It has been shown that some of the greatest wind energy potential resides in regions of topography. The problem is that most topography is covered by vegetation. Through their simulations of turbulent flow over hills that are both bare and forested, they are providing guidance as to the turbulence characteristics likely to be encountered in forested-hill environments. Due to maintenance costs, current turbine manufacturers and wind farm developers are unwilling to risk the potential damage associated with the increased turbulence intensities induced by forests. This research will lead to turbines designed around this regime and will ultimately expand wind farm resources both nationally and internationally.

The Whole Atmosphere Community Climate Model (WACCM)

The Whole Atmosphere Community Climate Model (WACCM) extends from the surface to ~ 150 km. This model builds on NCAR's Community Climate Model, version 3 (CCM3) and includes additional physics such as parameterizations of radiative heating, molecular diffusion, and ion drag in the middle and upper atmosphere. This model hence offers a more complete modeling system as compared to the CCM as it allows for examination of effects of the solar cycle & feedbacks of stratospheric chemistry and dynamics on the earth's climate. Due to the extensive computational domain, this model in its current state is not well suited for numerous climate sensitivity studies; however, with increasing computer power, this model is likely to become the model of choice for climate simulations in the next 10 years.

Note: A top boundary of ~ 20 km is depicted for the CMM on the slide. The CCM now actually extends closer to 40 km, however the resolution in the region btw. 20 – 40 km is very coarse, and hence it can not be trusted in that region.

One of the newest additions to WACCM is a new way of representing convectively generated gravity waves. In previous versions of the model (and in most other GCMs), gravity waves are specified to be distributed uniformly, at all times and at all latitudes – it's virtually a FIXED momentum source. Such a representation did not allow for interaction with the lower atmosphere and hence did not allow for feedbacks of changing tropospheric climate through gravity waves on the middle/upper atmosphere.

The new representation of gravity waves links gravity wave properties to the properties of underlying convection and hence produces more realistic and physically based forcing due to convectively generated gravity waves in the stratosphere and mesosphere (Convection is the main gravity wave source in the tropics). This is important for chemical and dynamical feedbacks between the atmospheric layers: as gravity waves propagate upwards and break, they deposit momentum to the mean flow. This momentum contributes to the driving of the stratospheric transport circulation, which for example transports ozone from the tropics to the polar region.

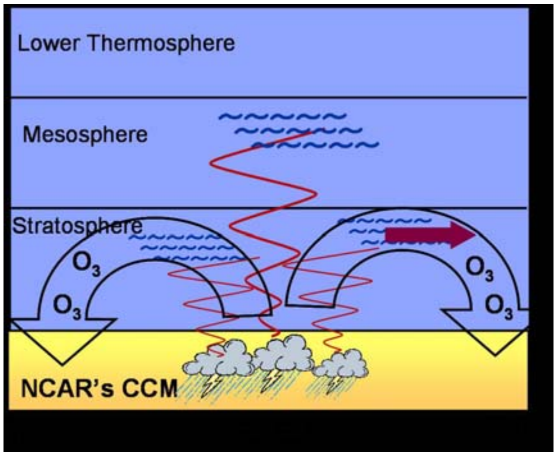

Note: In mid-latitudes, frontal systems are believed to be the major GW source – an interactive GW source spectrum parameterization is being implemented for that GW source this month (Feb 2005).

Discovery of TrES-1 and Subsequent Observation of Thermal Emission

The STARE Project (STellar Astrophysics & Research on Exoplanets), supervised by Dr. Tim Brown of HAO, uses a small-aperture telescope to search for planets orbiting other stars. The method relies on the edge-on alignment of the extra-solar system so that transits can be detected. A transit occurs when a planet passes between its star and the Earth, causing a slight dimming of the star's light. The planet itself is not seen directly, but inferred by the shape of the light curve.

In August of 2004 TrES-1, a giant planet orbiting a Sun-like star, was discovered using observations from the STARE instrument, a member of TrES (Trans-Atlantic Exoplanet Survey), a network of three small-aperture telescopes (STARE is located in the Canary Islands; Sleuth at Mount Palomar, California; and PSST at Lowell Observatory, Arizona). The planet is slightly larger than Jupiter with only ¾ of its mass. It has an orbital period of 3 days and is only 3.7 million miles from its star, which means it is very hot.

After the confirmation of TrES-1 as a transiting planet, Dr. David Charbonneau (formally of the STARE team, now of the Harvard-Smithsonian Center for Astrophysics and a member of the TrES Network with Sleuth) applied for, and received, observing time with the Spitzer Space Telescope. Observations were made in the infra-red while TrES-1 passed behind its parent star. Since the star produces most of its light in the visible portion of the spectrum and the planet re-radiates the energy it absorbs at longer wavelengths, the planet can be seen through the glare of the star by observing in the infra-red. This is the first ever direct observation of photons emitted by a planet orbiting another star. The measured thermal emission can then be used to infer the effective temperature of the planet, in this case approximately 1100K.

Transit observations such as these continue to provide a wealth of discovery not possible with other planet-search methods.

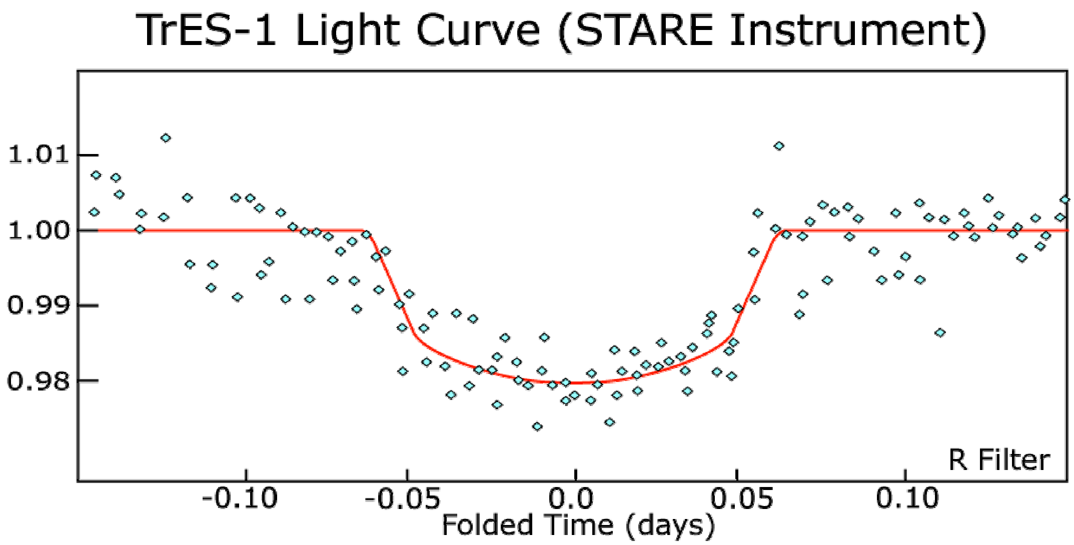

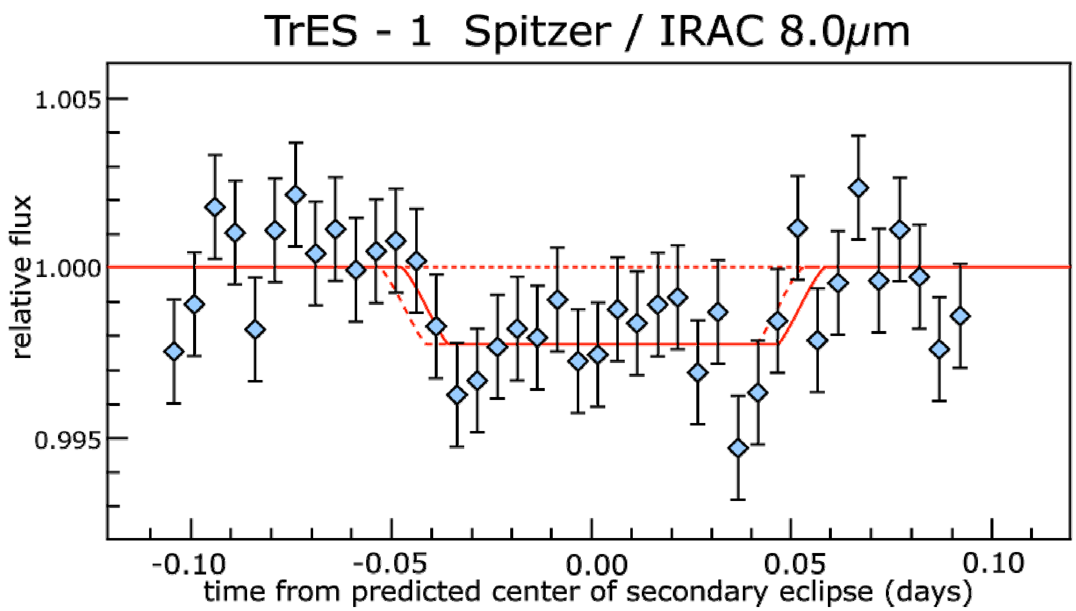

Role of subadiabatic tachocline for differential rotation

Even though details of the solar differential rotation are known through helioseismology to a large extent, theoretical approaches have still problems to explain the observed pattern. Differential rotation has been addressed by mainly two approaches in the past: 3D full sphere simulations of compressible convection and axisymmetric meanfield models that parametrize processes on the convective scale (turbulent diffusivities, turbulent angular momentum transport). 3D simulations were successful in predicting the correct amplitude of the differential rotation, however the profile is still closer to the Taylor-Proudman state with cylindrical differential rotation than to the observed pattern (isolines of Omega show an inclination of about 25 deg with the axis of rotation). Axisymmetric meanfield models recently showed that solar like differential rotation is possible if rotational anisotropy of the convective energy flux is taken into account that leads to a temperature difference of a few K between pole and equator (Kueker & Stix 2001, A&A, 366, 668 and references therein). M. Rempel developed a meanfield model for differential rotation in order to address the specific question if a subadiabatic tachocline, in conjunction with turbulent heat conductivity within the convection zone and overshoot region, can break the Taylor-Proudman constraint which requires a differential rotation constant on cylinders in case of an isentropic stratification. It was found that the entropy perturbation generated in the subadiabatic tachocline is significant compared to other sources (e.g. rotational anisotropy of the convective energy flux) and can be sufficient to explain the observed deviations from the Taylor-Proudman-state, if the contribution of the convection zone is more less neutral. If a non-adiabatic convection zone is considered, it is required that roughly the lower 40% to 50% of the convection zone are subadiabatic (due to non-local convection effects), otherwise additional effects like anisotropic heat transport are required to explain the observed differential rotation.

The meridional flow predicted by this approach shows in general a counter clockwise flow (if the radial angular momentum flux is negative), which is observed through helioseismology in the upper half of the convection zone. Such a flow is favorable for flux-transport dynamo models, where the equatorward meridional flow at the base of the convection zone ensures the equatorward propagation of magnetic activity through the solar cycle.

Combination of the differential rotation model with a meanfield dynamo model allows to address the feedback of the Lorentz force on differential rotation and meridional flow ("dynamic" flux-transport dynamos as opposed to "kinematic" flux-transport dynamos, where meridional flow and differential rotation are fixed and only the induction equation is solved).

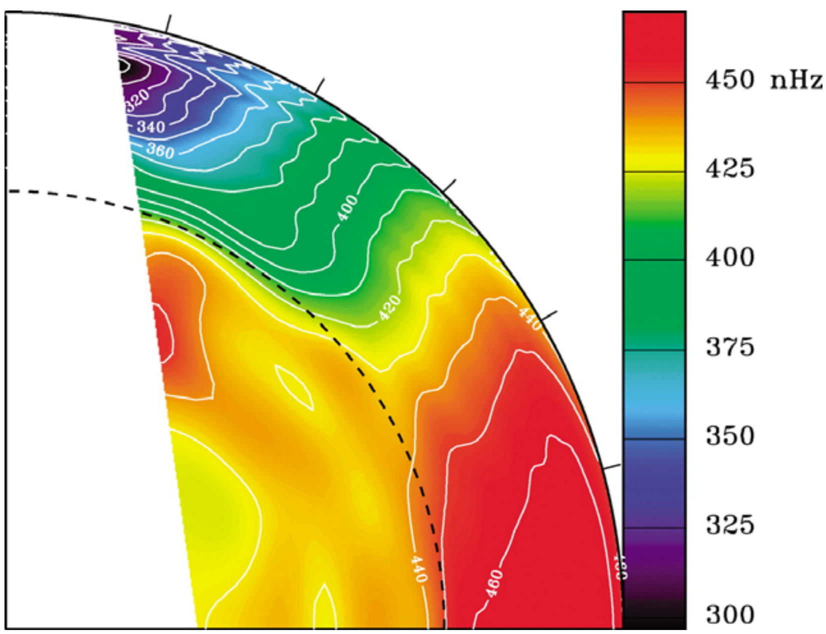

Observed DR (Schou et al. 1998)

Coronal Magnetism

The solar corona is a magnetically dominated system. The magnetic fields control coronal dynamics, coronal heating, and are responsible for space weather phenomena. With support from the NCAR Strategic Initiative on Coronal Magnetism, we have constructed the Coronal Multi-channel Polarimeter (CoMP) which is a filter-based polarimeter designed to provide quantitative measurements of magnetic fields in the solar corona. It measures the polarization properties of the coronal FeXIII emission lines at 1074.7 and 1097.8 nm and the chromospheric HeI emission line at 1083.0 nm. The CoMP is based on a four-stage birefringent filter and produces images at two wavelengths simultaneously. The strength of the line-of-sight (LOS) component of the magnetic field is inferred from the circular polarization, and the plane-of-sky direction of the magnetic field is inferred from the linear polarization. The instrument also provides a measurement if the LOS velocity as well as a measure of the plasma density.

The CoMP instrument resides on the 20-cm One Shot coronagraph of the National Solar Observatory at Sacramento Peak, New Mexico. It began operating in January of 2004.

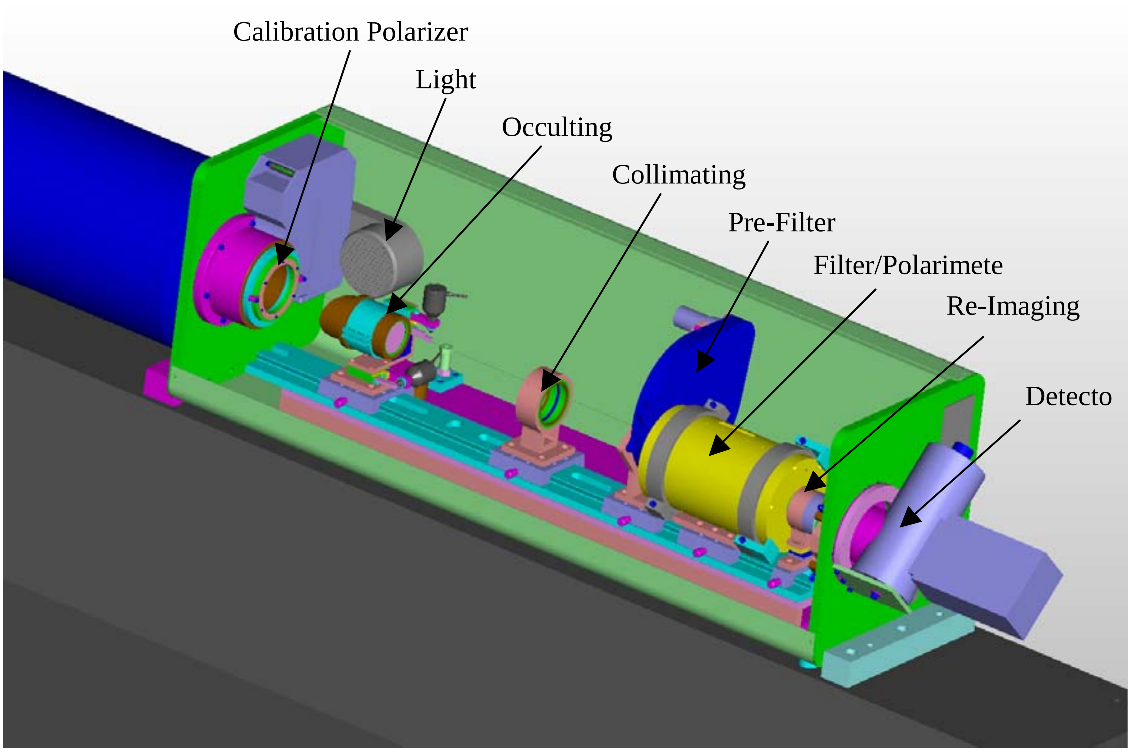

These three images below show the brightness, magnetic field strength, and Doppler velocity of an erupting solar prominence taken with the CoMP on March 9, 2004 in the HeI 1083 nm emission line. Positive and negative polarities of magnetic fields are indicated by the yellow and white colors of the middle image, while velocities directed towards and away from the observer are indicated by the blue and red colors of the rightmost figure.

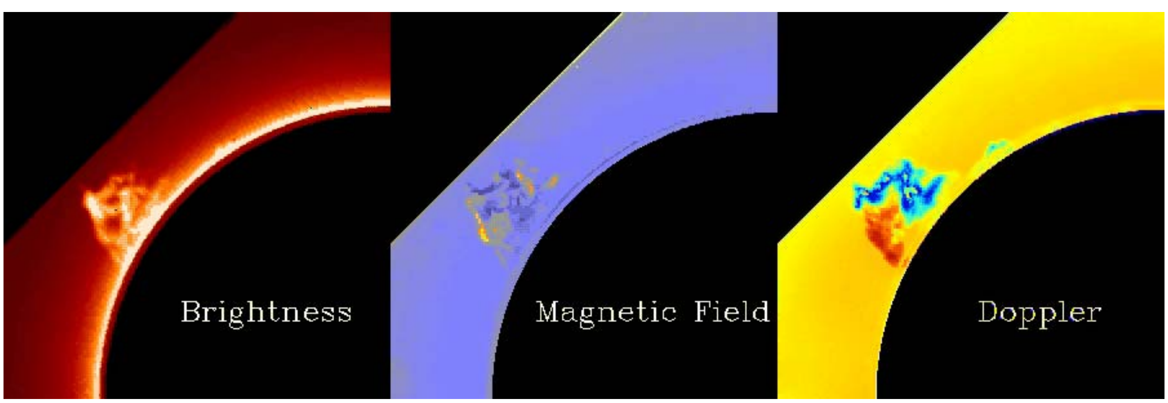

The six images show the inferred coronal properties on 21 April 2005 as observed in the FeXIII coronal emission line at 1074.7 nm.

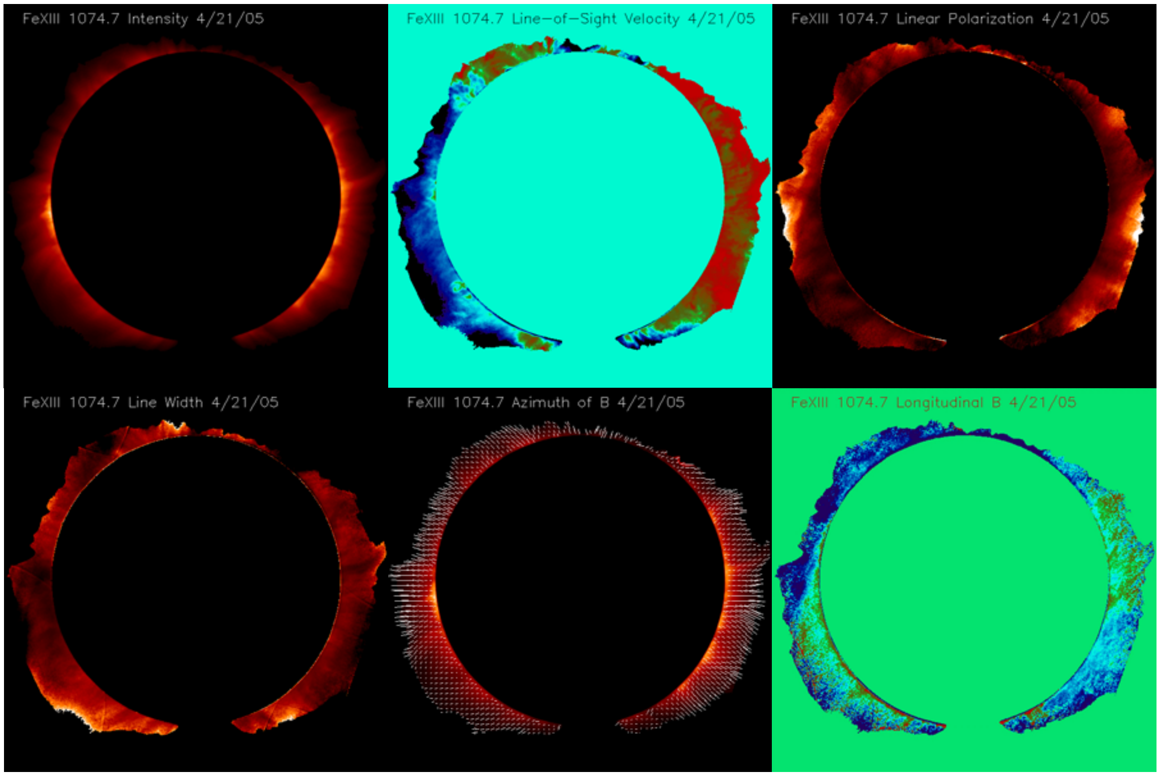

Additional Highlights:

Abrupt Climate Change in CCSM3, Bette Otto-Bliesner, Carrie Morrill, Bruce Briegleb, and Esther Brady

The National Research Council comments that abrupt climate changes can occur when the climate system surpasses a threshold. There are numerous examples in the paleoclimate record that indicate that the climate system has changed rapidly, in a matter of decades to a century, and dramatically, temperature changes of 5-10°C and precipitation changes of 50%. A marine core record in the Cariaco Basin off the coast of Venezuela (Figure 1) shows several prominent drying events over the last 20,000 years, including one starting about 17 ky BP and lasting about 1500 years (Heinrich Event 1, H1) and another occurring about 8200 yr BP and lasting 200 years (the 8.2 event). H1, when the Earth was still in a glacial state, has been associated with significant iceberg discharge into the North Atlantic and a shutdown of the North Atlantic thermohaline circulation (THC) (McManus *et al.*, 2004). The 8.2 event, during our current interglacial, has been associated with a large outburst flood into the Hudson Bay as the last remnants of the North American ice sheet melted rapidly (Clarke *et al.*, 2003).

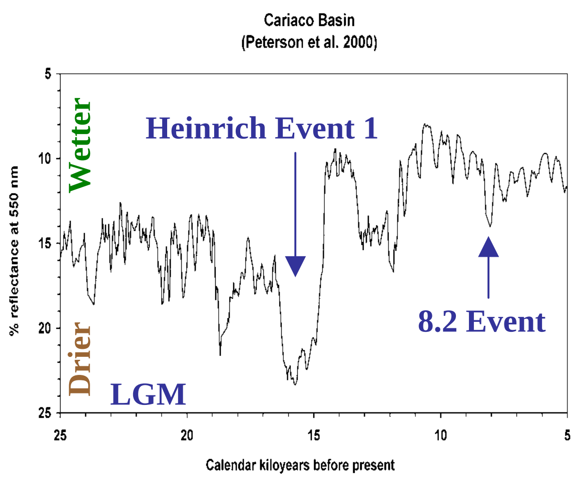

Figure 1. Marine core record from the Cariaco Basin showing measured reflectance as a proxy for precipitation/runoff from 25 to 5 ky BP. (Peterson et al., 2000)

Past abrupt climate changes have occurred with a variety of forcing. Geologic records for the H1 and 8.2 events indicate anomalous freshwater impulses into the North Atlantic, thus allowing testing of this mechanism in the NCAR Community Climate System Model (CCSM). Regional responses to a large freshwater forcing, 1 Sv for 100 years into the North Altantic from 50-70°N, proposed by CMIP for present-day, are investigated for both the glacial climate of H1 and the interglacial climate of the 8.2 event. In both scenarios, the North Atlantic climate simulated by CCSM responds dramatically, with an almost complete shutdown of the THC, cooling in excess of 12°C, and equatorward expansion of sea ice. The rates of change differ for the glacial cold versus interglacial warm background climate states on which the freshwater perturbation is applied, with the THC decreasing more rapidly but the North Atlantic sea ice increasing less rapidly for the 8.2 event as compared to the H1 event.

Changes associated with freshwater perturbations applied in the CCSM are not confined to the North Atlantic but are propagated remotely by the atmosphere and ocean. In the CCSM with the CMIP freshwater perturbation, precipitation in the Cariaco Basin decreases by 50% in the first 50 years of the freshwater forcing, remains low during the remainder of the forcing, and then gradually recovers after the freshwater forcing is removed (Figure 2). The CCSM results confirm proxy record interpretations of a southward shift of the

Intertropical Convergence Zone during the 8.2 event. Freshwater perturbations that more realistically model the size and length of the 8.2 outburst will be completed to determine if CCSM adequately simulates details of the record of this past abrupt change.

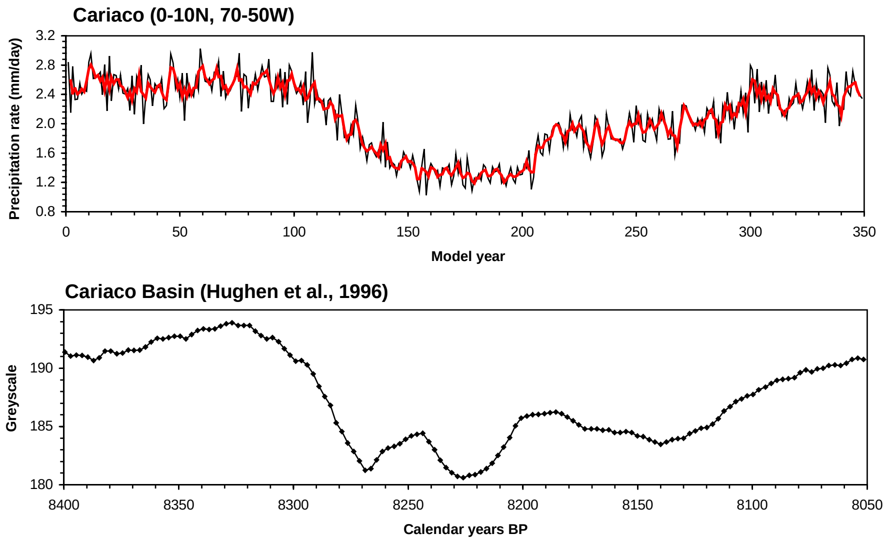

Figure 2. Time series of (top) precipitation rate predicted by CCSM3 for Cariaco region for 8200 years BP with freshwater perturbation of 0.1Sv applied in North Atlantic for years 100-199, and (bottom) greyscale as a proxy for precipitation/runoff measured in the Cariaco basin from 8400 to 8050 years BP. (Hughen et al., 1996)

References:

Clarke, G. K. C., D. Leverington, J. T. Teller, and A. S. Dyke, 2003: Superlakes, megafloods, and abrupt climate change. *Science*, **301,** 922-923.

Hughen, K. A., J. T. Overpeck, L. C. Peterson, and S. Trumbore, 1996: Rapid climate changes in the tropical Atlantic region during the last deglaciation. *Nature*, **380,** 51-54.

McManus, J. F., R. Francois, J.-M. Gherardi, L. Keigwin, and S. Brown-Leger, 2004: Collapse and rapid resumption of Atlantic meridional circulation linked to deglacial climate changes. *Nature*, **428,** 834-837.

Peterson, L. C., G. H. Haug, K. A. Hughen, and U. Rohl, 2000: Rapid changes in the hydrologic cycle of the tropical Atlantic during the last glacial. *Science*, **290,** 1947-1951.

Grant Branstator's use of the fluctuation-dissipation theorem

Working with Andrew Gritsoun and Valentin Dymnikov of the Russian Academy's Institute for Numerical Mathematics, Grant Branstator has used the fluctuation-dissipation theorem to construct a linear operator that estimates the response of an early version of NCAR's CCM to steady forcing. Cecil Leith first pointed out that the atmosphere approximately satisfies the conditions of the theorem making it possible to estimate its response to forcing without knowing the governing equations. Rather the response operator can be found simply by gathering statistics of the undisturbed system. Calculations performed by Branstator and colleagues confirm this as the attached example demonstrates. In this calculation the average upper tropospheric streamfunction response of the GCM to a heat source on the equator is compared to the response as given by the fluctuation-dissipation operator. From this example the accuracy of the operator is apparent. Given this success, it is now possible to answer questions in which an exhaustive, systematic forcing of the system is required. For example one might determine the most efficient way of counteracting global warming or the best way to suppress rainfall over India.

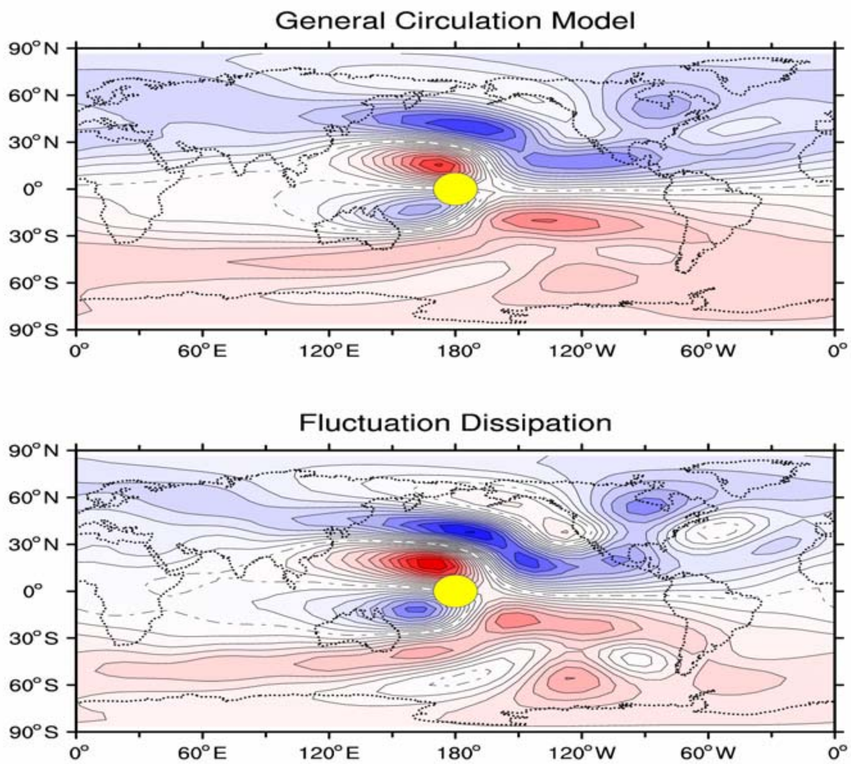
General Circulation Model
Fluctuation Dissipation
90° N
60° N
30° N
0°
30° S
60° S
90° S
60° E
120° E
180°
120° W
60° W

Tropical Variability Task Team

Both the CCSM Advisory Board and the CGD Advisory Committee have placed the highest priority on improving of longstanding biases in the CCSM class of models. In response, a Tropical Variability Task Team was formed to tackle the foremost of these biases. The first step was to produce the best possible equatorial ocean component, compared to observations. The success is demonstrated by the very favorable comparison of a fully coupled simulation relative to a data assimilation product used for initializing seasonal to inter-annual forecasts. In particular the strength of the Undercurrent and the eastward subsurface jets at ± 8° latitude are superior in the fully coupled case. These flows supply water to the eastern ocean boundaries where the largest surface temperature biases are found. In order to develop the jets, model developments were needed to enable the instability mechanism associated with Tropical Instability Waves. Step 2 will be to couple this ocean to an improved atmosphere.

Zonal Velocity 10ºS - 10Nº

Observed

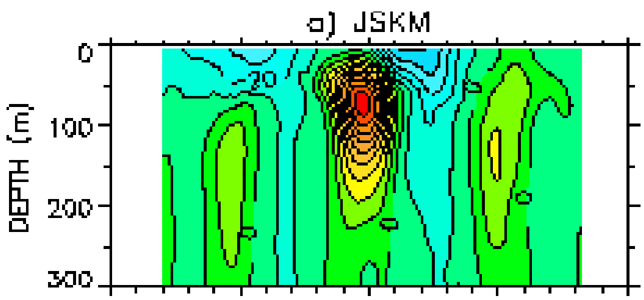

Data Assimilation

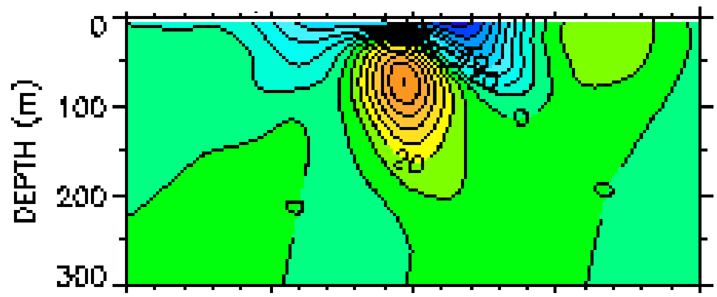

Fully Coupled

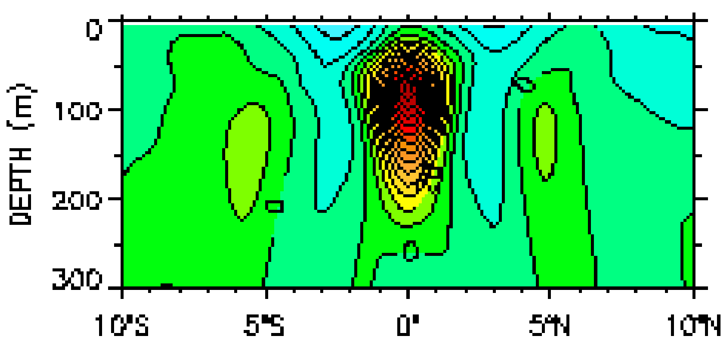

Water Vapor

It is only a small component of the atmosphere, accounting for 1.2×10^{16} kg, or 2.4 hPa in terms of surface pressure and thus about 0.24% of the atmosphere as a whole. Yet it is vital to climate and how it varies and changes. Water vapor is the most important greenhouse gas on the planet and accounts for about 60% of the current greenhouse effect, warming the planet enough to make it habitable. It provides the moisture that is captured by all weather systems to produce clouds and precipitation (rain and snow). It changes rapidly from hour to hour, and year to year, and its changes are vital for climate change as it provides the strongest positive feedback in the climate system. For instance, a doubling of carbon dioxide in the atmosphere from human fossil fuel burning, would increase global mean temperatures by about 1.2°C, but increased evaporation and water vapor roughly doubles that value.

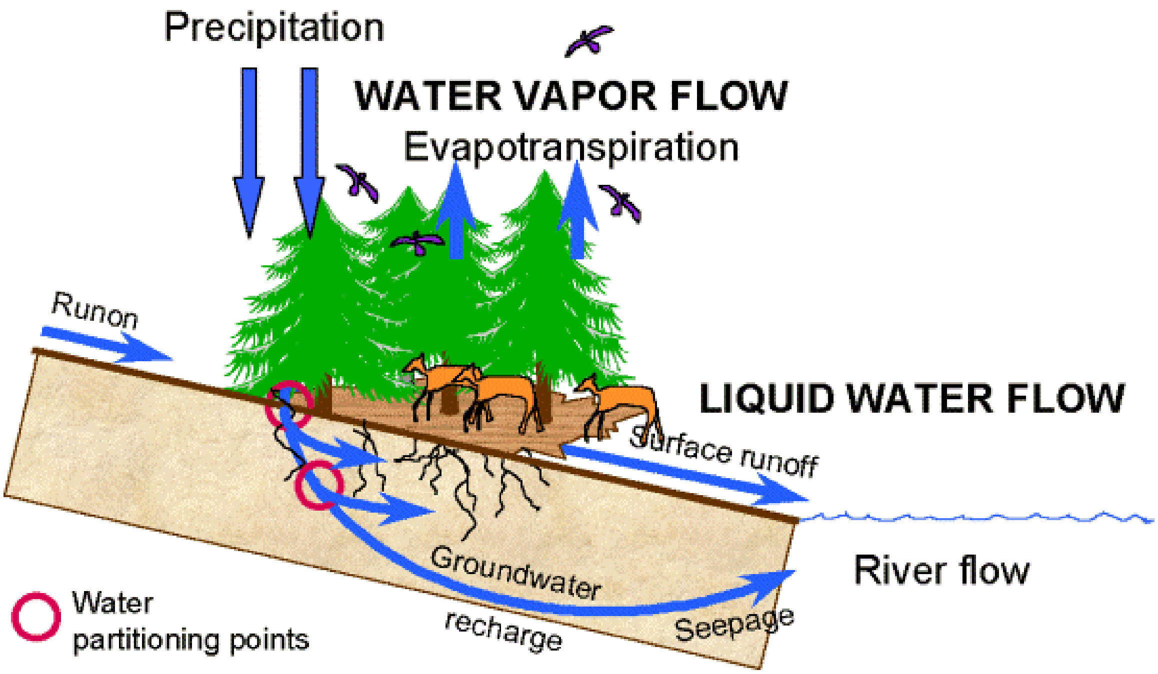

Figure from: Rockström, J., L. Gordon, C. Folke, M. Falkenmark, and M. Engwall. 1999. Linkages among water vapor flows, food production, and terrestrial ecosystem services. Conservation Ecology **3**(2): 5. [online] URL: http://www.consecol.org/vol3/iss2/art5/

In spite of its importance, changes in water vapor are poorly known. Measurements are difficult, and only since 1988 are values reliable over the ocean as new microwave measurements from SSM/I have come available.

Scientists in CAS have carefully evaluated many observations and datasets on water vapor and come up with new definitive answers on its mean, variability and trends.

See Trenberth, K. E., J. Fasullo, and L. Smith, 2005: Clim. Dyn.DOI 10.1007/s00382-005-0017-4. http://www.cgd.ucar.edu/cas/trenberth.papers/waterVapTrendsCoCDr.pdf

Precipitable water variability for 1988–2001 is dominated by the evolution of El Niño and especially the structures that occurred during and following the 1997–98 El Niño event. The evidence from SSM/I for the global ocean suggests that recent trends in precipitable water are generally positive and, for 1988 through 2003, average 0.40±0.09 mm decade^{-1} or 1.3±0.3% decade^{-1} for the ocean as a whole, where the error bars are 95% confidence intervals. Over the oceans, the precipitable water variability relates very strongly to changes in SSTs, both in terms of spatial structure of trends and temporal variability (with a regression coefficient for 30°N–30°S of 7.8% K^{-1}) and is consistent with the assumption of fairly constant relative humidity. These relationships allow estimates of changes in water vapor for the 20th Century to be about 5% over the global oceans, and this indeed suggests a radiative forcing equivalent to that of carbon dioxide increases.

At the same time, the increasing abundance of water vapor fuels stronger storms and makes for heavier rainfall events, which is also observed to be happening around the world.

This research by CAS scientists is not only important scientifically but also inpractical terms as to how the climate, precipitation and water resources change.

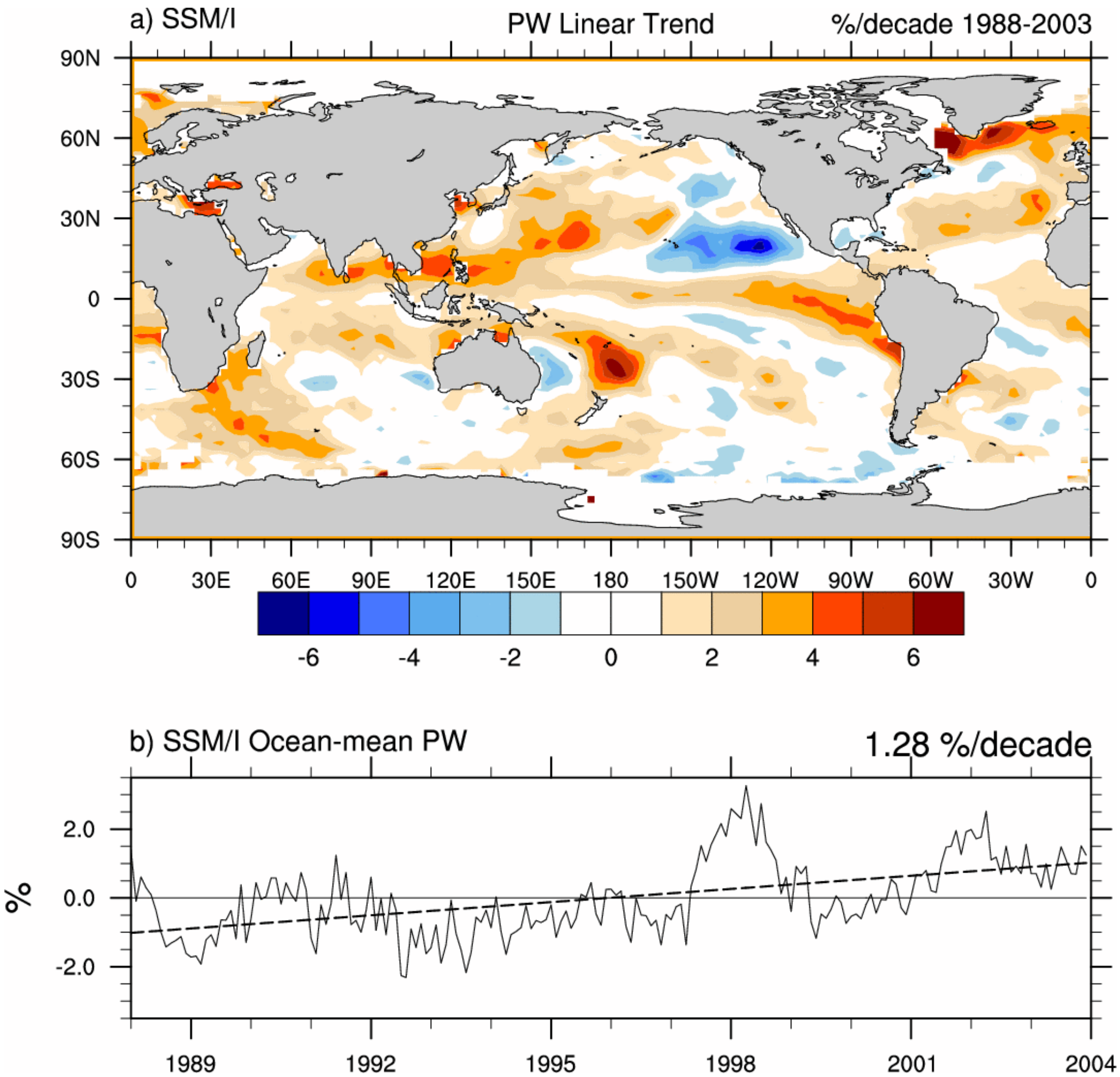

Fig. 11. Linear trend in precipitable water for 1988–2003in %/decade and the time series for the integral over the global ocean, which has a linear trend of 1.3 mm/decade.